ACS OMEGA

http://pubs.acs.org/journal/acsodf

Article

Global Mie Scattering: Polarization Morphologies and the Underlying Topological Invariant

Weijin Chen,[‖] Qingdong Yang,[‖] Yuntian Chen,[*] and Wei Liu[*]

Cite This: *ACS Omega* 2020, 5, 14157−14163

Read Online

ACCESS | Metrics & More | Article Recommendations

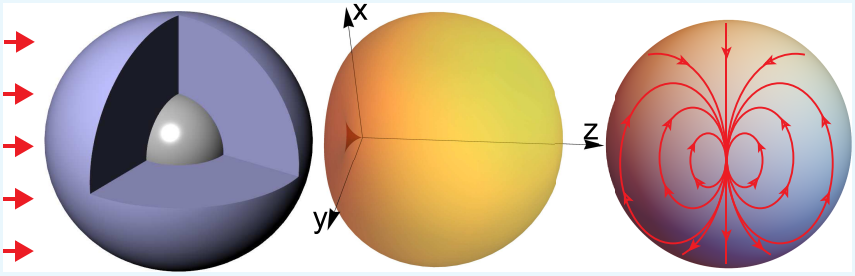

ABSTRACT: In various subdisciplines of optics and photonics, Mie theory has been serving as a fundamental language and playing indispensable roles widely. Conventional studies related to Mie scattering largely focus on local properties such as differential cross sections and angular polarization distributions. Though spatially integrated features of total cross sections in terms of both scattering and absorption are routine for investigations, they are intrinsically dependent on the specific morphologies of both the scattering bodies and the incident waves, consequently manifesting no sign of global invariance. Here, we propose a global Mie scattering theory to explore topological invariants for the characterization of scatterings by any obstacles of arbitrarily structured or polarized coherent light. It is revealed that, independent of distributions and interactions among the scattering bodies of arbitrary geometric and optical parameters, in the far field, inevitably, there are directions where the scatterings are either zero or circularly polarized. Furthermore, for each such singular direction, we can assign a half-integer index and the index sum of all those directions are bounded to be a global topological invariant of 2. The global Mie theory we propose, which is mathematically simple but conceptually penetrating, can render new perspectives for light scattering and topological photonics in both linear and nonlinear regimes and would potentially shed new light on the scattering of acoustic and matter waves of various forms.

INTRODUCTION

The seminal problem of light scattering by particles and the associated Mie theory has been pervasive in every subject of photonics, laying the foundation not only for studies and applications in optics and physics[1−3] but also those in many other interdisciplinary fields including even biology and medicine.[4,5] Conventional studies based on Mie theory concentrate on properties that can be roughly divided into two categories: overall integrated ones such as total absorption, scattering, and extinction cross sections; and local ones such as differential scattering cross sections and angular polarization distributions. Mie theory and those scattering properties broadly underlie various topics of nanophotonics, especially the new concepts and the phenomena of cloaking and invisibility,[6] superscattering,[7,8] and Kerker scattering and its generalized forms,[9,10] giving birth to and further expanding the field of Mie-tronics that largely originates from the interferences of radiating multipoles of different orders and natures.[11−13]

Besides the rapid progress relying on Mie theory in various directions, photonics, at the same time, has gained great momentum through incorporating novel topological concepts.[14,15] New topology-related ideas from condensed matter physics and other branches of physics have rendered extra degree of freedom for manipulations of light−matter interactions, through comprehensive exploitations of topological properties that are globally bounded.[14,15] For the classical scenario of light scattering by arbitrary obstacles, at first glance, the identification of globally invariant properties seems to be out of reach. This is simply due to the fact that both the aforementioned overall and the local scattering properties are intrinsically dependent on geometric and optical parameters of the specific scattering bodies, their distribution patterns, and the cross interactions.[1,2] Moreover, those scattering features are also dependent on the morphologies

Received: April 21, 2020
Accepted: May 18, 2020
Published: June 2, 2020

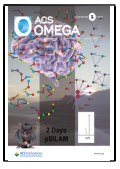

https://dx.doi.org/10.1021/acsomega.0c01843
ACS Omega 2020, 5, 14157−14163

of the incident waves, especially their spatial and polarization contextures.[3] Apart from those seemingly insurmountable difficulties, recently both local and globally invariant topological features have been revealed for radiating electromagnetic multipoles of arbitrary orders, revealing a hidden dimension of Bloch modes in periodic structures and their topological charges.[16,17] As essential entities in Mie theory, it is well known that electromagnetic multipoles serve as an orthogonal and complete basis for radiation expansion of any sources. As a result, it is natural to expect that the same topological idea can be extended to Mie scattering configurations with arbitrary finite obstacles and any coherently polarized incident waves.

In this work, we propose global Mie scattering theory to explore topological properties that are globally invariant for arbitrary Mie scattering configurations. Regardless of the specific morphologies of both the incident waves and the obstacles, the scatterings can always be mapped on the momentum sphere as tangent (transverse) fields perpendicular to the scattering directions. For such continuous tangent fields on a two-dimensional spherical surface, the fundamental Poincaré–Hopf theorem can be directly applied.[18,19] As for our physical problem of Mie scattering of any specific configurations, this mathematical theorem secures the following two facts: (i) Across the momentum sphere, despite some obviously trivial cases such as invisibility of zero total scattering, there must be isolated directions along which the scattering is either zero or circularly polarized; (ii) For each of such singular directions, a half-integer index can be assigned and the index sum of all those directions is bounded to be 2, which is the Euler characteristic of the momentum sphere. Our mathematically simple while conceptually deep global Mie theory has effectively blended two sweeping concepts of Mie scattering and global topology of Euler characteristics and singularities.[18,19] Considering the foundational roles of Mie theory and the recent rapid pervasion of topological concepts throughout photonics, we believe that the proposed global theory can further accelerate the interplay of photonics and topology. This can hopefully make possible more flexible controls of light–matter interactions in both linear and nonlinear regimes, with broad implications for molecular scattering and optical activity studies, and even for waves of other forms.

RESULTS AND DISCUSSION

For the general case of light scattering by arbitrary finite obstacles, regardless of the shapes and optical properties of each individual scattering body, and how different scattering bodies are clustered, the scattered fields are continuously distributed among different directions on a momentum sphere parameterized by θ and ϕ (see Figure 1a for the momentum sphere in a spherical coordinate system). Moreover, since in the far field the scattering is purely transverse with both electric and magnetic fields perpendicular to the scattering directions (denoted by $\hat{\mathbf{e}}_r$), the fields can be viewed as continuous tangent fields on the $\hat{\mathbf{e}}_\theta$–$\hat{\mathbf{e}}_\phi$ plane.

A simple scenario to start with is that all of the scattered fields are linearly polarized throughout the momentum sphere, on which the tangent electric and magnetic fields can be fully represented by vector fields. As for such continuous vector field on the momentum sphere, the Poincaré–Hopf theorem[18,19] requires that there must be isolated directions where there is no scattering (the vector field and also the total

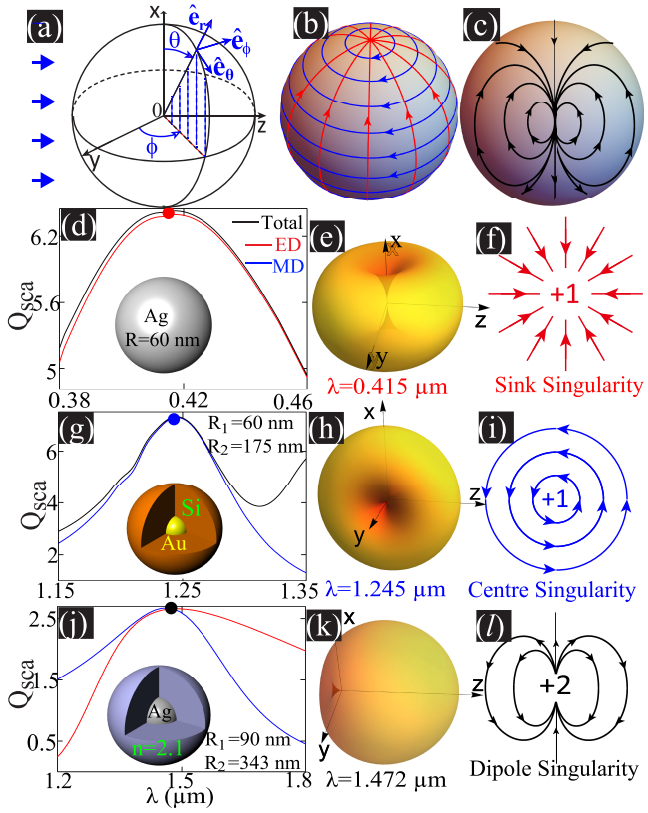

Figure 1. (a) Momentum sphere parameterized by both Cartesian and polar coordinates, with the associated orthonormal basis vectors $\hat{\mathbf{e}}_\theta$, $\hat{\mathbf{e}}_\phi$, and $\hat{\mathbf{e}}_r$ specified. Other parameters have their usual meaning. On the momentum sphere, continuous tangent vectors exist with two singularities of Poincaré index +1 (located on poles) in (b) and one singularity of Poincaré index +2 in (c). (d, g, j): Scattering efficiency spectra (both total and dipolar partial ones are included) for homogeneous or core–shell spherical particles (see insets) with the resonant positions indicated by dots. The scattering patterns at those positions are shown in (e), (h), and (k), respectively. Vectorial field patterns close to singularities are shown in (f), (i), and (l), the Poincaré indices of which are also specified.

intensity are strictly zero). Those directions correspond to singularities of vector fields (vectorial singularities denoted by **V** points in this work), and for each singularity, an integer Poincaré index (or equivalently winding numbers of the vector fields that trace out the closed contour[19]) can be assigned. All across the momentum sphere, the sum of Poincaré indices for all singularities is bounded to be 2, which is the corresponding Euler characteristic.[18,19] In Figure 1b, we show two sets of well-known vector fields consisting of latitude (θ is constant) and longitude (ϕ is constant) vectors. For both sets, there are two singularities locating on the poles (θ = 0 or π), each of Poincaré index +1 with their sum being 2, as required by the Poincaré–Hopf theorem. We have also shown in Figure 1c another set of less well-known but equally important vector fields with only one singularity of Poincaré index +2, which is termed as a dipole singularity (the vectorial patterns close to the singularity are the same as those of a static electric dipole (ED)).[19]

The simplest scenario of everywhere linearly polarized scattering is that by an obstacle which can be viewed as a linearly oscillating electric dipole (ED). Rayleigh scattering with linearly polarized incident plane waves falls into this category.[1] In Figure 1d, alternatively, we show another example

https://dx.doi.org/10.1021/acsomega.0c01843
ACS Omega 2020, 5, 14157–14163

of plane wave scattering by an Ag sphere (radius R = 60 nm; permittivity adopted from ref 20) that supports surface plasmon resonances.[21] The plane wave is **x**-polarized and propagating along **z**, and the scattering spectra (scattering efficiency Q_{sca}, which is scattering cross section divided by the cross section of the sphere) in terms of both total and partial ED scatterings are summarized in Figure 1d. The geometric and optical properties of the scattering bodies can be found in the figure, as is the case for other scattering configurations throughout this work. As is shown, at the marked resonant position (the wavelength λ = 415 nm), there is ED scattering that is linearly polarized throughout the momentum sphere. The far-field scattering pattern (in terms of angular scattering intensity, as is the case throughout this work) at this spectral position is shown in Figure 1e, with their singularities locating at the poles, which coincide with the dipole oscillating direction. A simple analysis based on the formulas of dipolar scattered fields reveals that scattered magnetic and electric fields of the ED on the momentum sphere are exactly represented by those latitude and longitude vectors shown in Figure 1b, respectively.[22] The electric field patterns in the neighborhood of the singularities are shown in Figure 1f. Here, only the sink singularity of Poincaré index +1 at one pole is shown and the corresponding source singularity at the opposite pole can be directly obtained through flipping the orientations of all vectors, with the same index +1.[19]

The duality of Maxwell equations guarantees that the scattering patterns of an ED and a magnetic dipole (MD) would be identical, with the interchange of electric and magnetic terms (including both the dipolar moments and vector fields).[22] Figure 1g shows the scattering spectra of a Au−Si core−shell particle, where for the gold core, R_1 = 60 nm and permittivity taken from ref 20, and for the silicon shell, R_2 = 175 nm and permittivity taken from ref 23. At the resonant position (λ = 1245 nm), a pure MD can be exclusively obtained.[24,25] Apart from a $\pi/2$ rotation about the **z** axis (since the MD moment is along the **y** axis parallel to the incident magnetic field, while the ED moment is along the **x** axis parallel to the incident electric field), the scattering pattern (shown in Figure 1h) is the same as that of an ED, and electric field patterns close to the singularities (center singularities located at ϕ = 0 and π with Poincaré index +1) are shown in Figure 1i. According to the duality principle, the patterns of tangent electric and magnetic fields of the MD are exactly the same as those of tangent magnetic and electric fields of the ED, respectively. They are respectively latitude and longitude vectors shown in Figure 1b, meaning that the magnetic field singularities of MD are source or sink singularities.

Another elementary case of linearly polarized scattering is the one that can be represented by vector fields shown in Figure 1c, with only one dipole singularity of Poincaré index +2. This type of field patterns is inaccessible to obstacles that support a single multipolar moment, the scattering of which is symmetric with at least two singularities. The simplest configuration to achieve this is based on an in-phase overlapping of an ED and an MD of the same magnitude,[10,16,26] and this ED−MD pair is also termed as a dynamic Kerker dipole.[9,10,16] Figure 1j shows the scattering spectra of a core−shell particle [the core is Ag of radius R_1 = 90 nm and the shell is dielectric (refractive index 2.1) of radius R_2 = 343 nm], which confirm that at the marked resonant position (λ = 1472 nm), the ED and MD overlap and the particle can be treated as a Kerker dipole. The scattering pattern at the overlapping resonant position (see Figure 1k) exhibits a dipole singularity at the minus **z** backward direction, with the vector field pattern close to it shown in Figure 1l, which is identical to that shown in Figure 1c.

To date, we have discussed only the simple scenario when the scattering is fully linearly polarized all across the momentum sphere. Nevertheless, it is well known that light is generally elliptically polarized, and the linear and circular polarizations are merely special cases.[22] For general scattering of elliptic polarizations, at any fixed temporal moment, we can treat the scattered fields as vector fields (as presented already in Figure 1), and then the conclusions drawn above for vectorial singularities of integer Poincaré indices can be directly applied. However, the vectors are rotating temporally for elliptic polarizations, meaning that the vector field patterns are constantly changing. To effectively characterize the evolving patterns and to further establish connections to experimentally measurable quantities that are time-averaged, static line fields should be introduced.[17,27−29] Intuitively, line fields are nonoriented vector fields, that is, lines without arrows.[27−29] Transversing a closed contour within vector fields would bring a vector back to itself with a fixed orientation, requiring that the overall rotation angle along the loop being an integer number of 2π and thus leading to integer Poincaré indices. While for line fields, since there is no orientation for each line, a half-integer number of 2π rotation is sufficient to bring the line field back to itself, resulting in half-integer Hopf indices.[27] The intrinsic singularities of vector fields are those of Poincaré indices $\pm$1, and other higher-index ones can be viewed as a singularity composite when multiple intrinsic singularities overlap with one another. The same principle is also applicable to line fields, but here the intrinsic singularities are those of Hopf indices $\pm$1/2. From this perspective, for both line and vector fields, the higher-index singularities are accidental, which can be simply decomposed into several intrinsic singularities through further perturbations.[18,19,27]

For electromagnetic waves, the widely constructed line fields for general elliptical polarizations consist of long axes of the polarization ellipses, which are also termed as polarization fields.[28,29] For linear polarizations, line fields can be directly constructed through removing the arrows of the vectors. Then, the vectorial singularities become line singularities automatically, with the Poincaré and Hopf indices equal to each other. For example, the vector fields (vectorial singularities) shown in Figure 1b,c would become line fields (line singularities) with the arrows removed, with the positions and indices of the singularities unchanged. For linearly polarized scattering, the vectorial singularities correspond to directions where the scattering is zero with integer Poincaré indices, while for elliptically polarized scattering, line singularities with half-integer Hopf indices correspond to directions of either zero scattering or circularly polarized scattering (denoted as **C** points). For both types of singularities, the long axis is not well defined.[28,29] Apart from those differences, the Poincaré−Hopf theorem is applicable to both vector fields and line fields.[18,19,27] Considering that the application of the theorem requires only the continuity of the scattered fields that has nothing to do with how the scatterings are induced and that there are two types of line singularities, it is easy to conclude the following for arbitrary scattering bodies in a homogeneous background: (i) There must be isolated singularities (singular directions on the momentum sphere) where the scattering is either zero or circularly polarized. (ii) The Hopf index sum of all of those

https://dx.doi.org/10.1021/acsomega.0c01843
ACS Omega 2020, 5, 14157−14163

singularities has to be 2. From the perspective of line fields, even intrinsic vectorial singularities of Poincaré index ±1 are not fundamental anymore, as they can be further separated, through adding perturbations of extra multipolar terms, into a pair of **C** points with opposite handedness and the same Hopf index of 1/2 or −1/2.[22,28,29] In contrast, intrinsic line singularities of index ±1/2 are fundamental and cannot possibly be further decomposed.

To further exemplify the aforementioned basic concepts and global topological invariance of line fields constructed from general elliptically polarized scattering, we show in Figure 2a

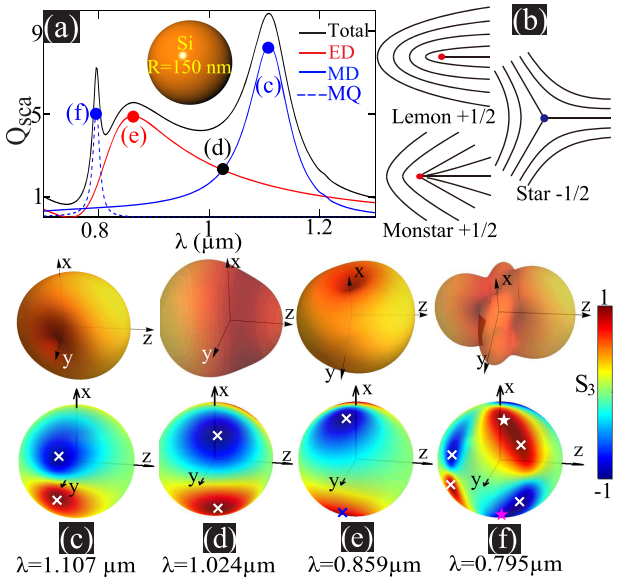

Figure 2. (a) Scattering efficiency spectra (both total and partial ones contributed by the ED, MD, and MQ are shown) for a silicon sphere of radius 150 nm. Three resonant (λ = 1107, 859, 795 nm) and one nonresonant (λ = 1024 nm) spectral positions are indicated. The scattering intensity patterns and Stokes parameter (S_3) distributions at those positions are shown correspondingly in (c)−(f), where **C** points are marked by crosses of Hopf index +1/2 or stars of Hopf index −1/2. Three typical line field patterns close to intrinsic singularities are shown in (b): Lemon and Monstar singularities of Hopf index +1/2 and Star singularity of Hopf index −1/2.

the scattering spectra of a silicon sphere of radius 150 nm. Besides the contributions from the ED and MD, that from the magnetic quadrupole (MQ) is also included. At each indicated position, besides the scattering patterns, we show also the distributions of Stokes parameter S_3 on the momentum sphere to identify the positions of **C**-point singularities (S_3 = ±1 corresponds respectively to left-handed and right-handed circular polarizations; S_3 = 0 corresponds to linear polarizations, as is the case throughout the momentum sphere in Figure 1) in Figure 2c−f.

For the primitive Mie scattering with linearly polarized plane waves and spherical particles, linearly polarized scattering all across the momentum sphere can be obtained when Mie scattering coefficients (a_m and b_m, where m is a positive integer) fulfill one of the following requirements:[1] (i) Only one coefficient is nonzero and (ii) the ratios between any two nonzero scattering coefficients are real. For the well-known two cases of ED and MD scattering discussed already, the first requirement is satisfied with $a_1 \neq 0$ and $b_1 \neq 0$, respectively, while for the scenario of Kerker dipole mentioned above, the second condition is met with $a_1/b_1 = 1$. Though in Figure 1 we have shown the results only at the resonant spectral positions, this criterion is generally applicable. For example, Rayleigh scattering occurs at the regime where $a_1 \neq 0$ and the scattering is far from the resonant position ($|a_1| \ll 1$). As a result, Rayleigh scattering with linearly polarized plane wave has a typical linear polarization pattern of an ED.

For the marked points shown in Figure 2a [including both resonant (λ = 1107, 859, 795 nm) and nonresonant (λ = 1024 nm) spectral positions], neither of the aforementioned two conditions is satisfied. This can be simply confirmed through direct calculations for ratios of the nonvanishing Mie scattering coefficients. The corresponding scattering patterns at those points render an alternative confirmation: there are no directions along which the scattering is zero (see Figure 2c−f). This is because, as we have argued above, if the scattering is everywhere on the momentum sphere linearly polarized, there must be directions of zero scattering (**V** points). As a result, the singularities must be **C** points along which the scattering is circularly polarized. Those line singularities are marked by crosses of Hopf index +1/2 or stars of Hopf index −1/2 on the S_3 distribution graphs shown in Figure 2c−f. At each position, only half of singularities are visible and the other half can be inferred from the symmetry of the scattering with respect to the **x**−**z** plane. We emphasize that the pseudo-scalar nature of chirality[22,30] means that each **C** point marked in Figure 2c−f has another unshown (on the other side of the sphere) imaging singularity partner with opposite handedness ($S_3 = \pm 1$) but the same Hopf index (mirror symmetry does not change the Hopf index of the singularity). The common feature of the three dipolar (both resonant and nonresonant) scattering cases (shown in Figure 2c−e, where there are no quadrupolar or higher-order multipolar contributions) is that there are four **C** points across the momentum sphere and each has a Hopf index of +1/2 with the sum being 2. For the last case with dominant MQ scattering (λ = 795 nm), on the momentum sphere, there are altogether 12 isolated singularities (only six are visible): four of Hopf index −1/2 (two of them are marked by stars) and eight of Hopf index +1/2 (four of them are marked by crosses), with the index sum being 2.

It is worth mentioning that, for both vectorial and line singularities, each index corresponds to infinitely many possible field patterns that are geometrically distinct while topologically equivalent in the neighborhood of the singularities.[28,29,31] In Figure 2b, we show only three typical line field patterns close to the intrinsic singularities of Hopf index of ±1/2, that is, Lemon and Monstar singularities of Hopf index +1/2 and Star singularity of Hopf index −1/2. The Lemon and Monstar singularities have the same Hopf index and thus topologically equivalent, meaning that they are smoothly interconvertible.[31,32] We further note that investigations into the scattering properties of dielectric particles from the perspective of line field and line singularities have been conducted before,[33] which nevertheless concentrate on the local properties, without revealing the global feature of unavoidable existences of singularities (isolated directions of zero or circularly polarized scattering) and the invariance of the index sum. This is understandable since previous studies were not performed within the general global framework of the Poincaré−Hopf theorem.

As mentioned already, our analysis based on the Poincaré−Hopf theorem has nothing to do with the shape of the scattering bodies (being them ideally spherical or not) or how

https://dx.doi.org/10.1021/acsomega.0c01843
ACS Omega 2020, 5, 14157−14163

those scattering bodies are clustered and interact with one another. As a next step, we turn to the geometrically less symmetric while widely celebrated structure of split ring resonators (SRRs) for further illustrations of the global Mie scattering. The SRRs investigated in this work are identical, geometric and optical parameters of which are the same as those in the experimental study: geometric parameters are specified in Figure 3a; they are made of gold, the permittivity

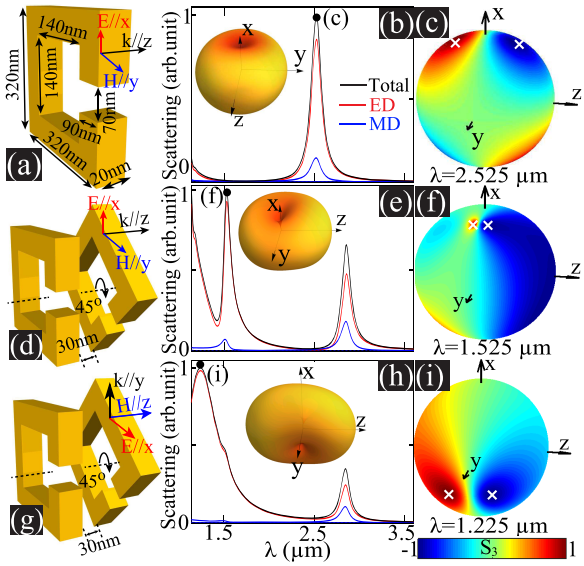

Figure 3. Linearly polarized plane waves scattered by an individual SRR in (a) or twisted SRR pairs in (d) and (g). All SRRs are identical with the geometric parameters specified in (a). The twisted pair consists of two **z**-coaxial SRRs with a 45° relative rotation and a 30 nm gap between them. The scattering spectra (normalized) are shown respectively in (b), (e), and (h). For each scattering configuration, a resonant position is marked (λ = 2.525, 1.525, and 1.225 μm), at which the scattering intensity patterns are included as insets. The S_3 distributions are shown respectively in (c), (f), and (i), and for all of them, there are four **C**-point singularities of Hopf index +1/2 (half of them are visible and marked by crosses), with the index sum being 2.

of which in our investigated spectral regime is given by the Drude model $\varepsilon(\omega) = 1 - \omega_p^2/\omega(\omega + i\omega_c)$, where $\omega_p \approx 1.37 \times 10^{16}$ Hz is the plasma frequency and $\omega_c \approx 4.08 \times 10^{13}$ Hz is the collision frequency.[34] We first study the widely employed configurations with linearly polarized incident plane waves shown in Figure 3a,d,g, including both an individual SRR and a twisted SRR pair (two **z**-axis-coaxial SRRs with a 45° relative rotation and a 30 nm gap, as shown in Figure 3d,g). The spectral regime examined is where there is a significant optically induced magnetic response that is foundational for the field of metamaterials, with the corresponding scattering spectra of each configuration shown in Figure 3b,e,h. For each case, we have marked a resonant position (λ = 2.525, 1.525, and 1.225 μm, respectively), at which the S_3 parameter distributions across the momentum sphere are shown respectively in Figure 3c,f,i. Similar to those shown in Figure 2, the none scenario manifests **V**-point singularities along which there are no radiations (see scattering intensity patterns included as insets of Figure 3b,e,h). This is natural, as we have already argued above, **V**-point singularities are accidental and would easily break up into intrinsic **C**-point singularities for general elliptically polarized scatterings. For each case, four intrinsic **C**-point singularities of Hopf index +1/2 (half of them are visible and indicated by crosses) are always present (see Figure 3c,f,i), with the index sum being always 2, as dictated by the Poincaré−Hopf theorem.

Though we have so far confined our discussions to the incidence of linearly polarized plane waves, our conclusion concerning the global topological properties is independent of not only scattering bodies but also the incident waves. Now we consider the same configuration of twisted SRR pair (as is shown in Figure 3d) that is widely employed to study the artificial optical activity[35,36] but switch the incident waves to circular polarizations. The scattering spectra shown in Figure 4a,c for incident waves of different handedness (left- and right-

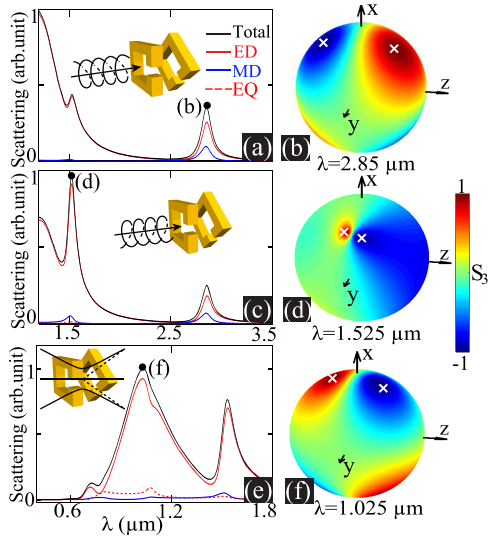

Figure 4. Scattering of left- and right-handed circularly polarized planes waves, and a Gaussian beam by the SRR pairs that are the same (see insets) as those studied already in Figure 3, with the spectra shown, respectively, in (a), (c), and (e). A resonant position is marked for each case (λ = 2.85, 1.525, and 1.025 μm), at which the S_3 distributions are shown, respectively, in (b), (d), and (f). For all scenarios, there are four **C**-point singularities of Hopf index +1/2 (half of them are visible and marked by crosses), with the index sum being 2.

handed, respectively) are distinct due to the chirality of the SRR pair. For each case, we have marked a resonant position (λ = 2.85 and 1.525 μm) at which the S_3 parameter distributions across the momentum are shown accordingly in Figure 4b,d. As is clearly demonstrated, despite the opposite handedness, for both cases, there are four intrinsic **C**-point singularities of Hopf index +1/2 (half of them are visible and marked by crosses). We further investigate the scattering by such an SRR pair of an x-polarized Gaussian beam, which propagates along the **z** axis with the beam waist radius 1.5 μm and the beam center coinciding with the geometric center of the SRR pair. Its scattering spectra are shown in Figure 4e with the presence of also an electric quadrupole (EQ). At the marked resonant position (λ = 1.025 μm), the corresponding S_3 parameter distribution in Figure 4f clearly manifests **C**-point singularities (two of four singularities are visible and marked; all with Hopf index +1/2), indicating that the global topological properties are preserved regardless of the spatial shape of the incident wave. We emphasize that here in Figures 3 and 4 we have investigated only the long-wavelength regime when there are only dominant lower-order multipolar (up to quadrupole) scattering. As for the larger-frequency regions

https://dx.doi.org/10.1021/acsomega.0c01843
ACS Omega 2020, 5, 14157−14163

with the emergence of higher-order multipoles, more singularities will be observed across the momentum sphere (harder to be directly visualized though; see, for example, Figure 2f). The index sum of all singularities is bounded to be 2, no matter how many multipoles are involved and how high the orders of the involved multipoles can be. This principle holds valid at any spectral positions including nonresonant ones (see, for example, Figure 2d), although in Figures 3 and 4, we have shown only the results at the resonant points where the scattering is stronger and easier to be measured.

CONCLUSIONS

Our work here has addressed a fundamental problem: For light scattering by arbitrary obstacles, is it possible to define globally invariant properties to characterize any scattering that is dependent on neither the scattering bodies nor the incident waves? Through a cornerstone theorem of global differential geometry, the Poincaré–Hopf theorem, we show that for arbitrary finite obstacle scatterings in a homogeneous background, there must be isolated singular directions where the scattering is either zero or circularly polarized. For both sorts of singularities, we can assign half-integer Hopf indices, and the index sum of all singularities has to be 2, which is the Euler characteristic of the momentum sphere. Since the Poincaré–Hopf theorem requires only the continuity of the tangent fields (i.e., transverse electromagnetic fields scattered to the far field for our specific problem), it cares nothing about how the fields are generated and thus the global properties we have revealed are generically independent of the specific scattering configurations. Here, for the first time, we have merged Mie scattering with global topological concepts, which can potentially nourish new perspectives for both conventional Mie scattering-related problems, such as optical resonators, metasurfaces, vectorial vortex beams, and so on, and the recently rapidly expanding field of topological photonics. Since scattering is a fundamental phenomenon for different branches of physics, which pervades not only electromagnetic waves but also waves of other natures, we believe our work also sheds new light on subjects such as acoustics, seismic studies, and other subdisciplines involving matter waves.

At the same time, we would like to point out the limitations of our work: (i) Here, we have confined our discussions to far-field scatterings, where the fields are transverse (tangent) and thus the Poincaré–Hopf theorem is directly applicable. In the near field however, the electromagnetic fields are not transverse anymore and the employment of the Poincaré–Hopf theorem requires that all radial terms of the fields are dropped, and then the conclusions we have drawn are still valid for arbitrary near-field scattered or radiated electromagnetic waves. (ii) Neither static vector fields nor line fields can be directly defined for partially polarized and/or incoherent light, and then the global principle we have discovered here is not directly applicable. (iii) Singularities in terms of either electric or magnetic fields (as we have done here) are not invariant under Lorentz transformations, and thus, for more general scenarios (such as scattering within a moving background, or the scattering body and the observer are in relative motion), the introduction of Riemann–Silberstein fields is necessary.[37,38] At the current stage, it is not clear whether or not it is possible to define invariant parameters to characterize scattering of those more general scenarios, which deserves further investigations from such a global perspective.

COMPUTATIONAL METHODS

For spherical particles (both homogeneous and core–shell ones), the scattering spectra (both total scattering and partial scattering from different multipolar components), angular radiation patterns, and Stokes parameter (S_3) distributions can be analytically calculated from the standard Mie theory.[1] With the scattered field distributions obtained close to the singularities, the indices (both Poincaré and Hopf ones) can be directly calculated through the approaches described in ref 39.

For nonspherical structures studied in this work, we employ a commercial software package COMSOL MULTIPHYSICS (https://www.comsol.com) to extract the scattered fields. With the extracted information, we can directly calculate the total scattering spectra, angular radiation patterns, and Stokes parameter distributions. For partial scattering spectra of different multipolar components, we conduct the spherical harmonic expansions of the extracted scattered fields to obtain all of the expansion coefficients: a_{nm} for electric multipoles and b_{nm} for magnetic multipoles.[40] With those coefficients, the total scattering can be accurately separated and attributed to different multipoles:[41] the scattering contributed by electric multipoles of order n is proportional to $\sum_{m=-n}^{m=n}(2n+1)|a_{nm}|^2$, and that contributed by magnetic multipoles is proportional to $\sum_{m=-n}^{m=n}(2n+1)|b_{nm}|^2$. For example, the scatting of ED and MD is proportional to $\sum_{m=-1}^{m=1} 3|a_{1m}|^2$ and $\sum_{m=-1}^{m=1} 3|b_{1m}|^2$, respectively, while the scattering of EQ and MQ is proportional to $\sum_{m=-2}^{m=2} 5|a_{2m}|^2$ and $\sum_{m=-2}^{m=2} 5|b_{2m}|^2$, respectively. We note that for the scenario of an incident Gaussian beam, we have subtracted the incident wave from the total extracted fields in COMSOL to calculate all of the scattering parameters.

AUTHOR INFORMATION

Corresponding Authors

Yuntian Chen − *School of Optical and Electronic Information and Wuhan National Laboratory for Optoelectronics, Huazhong University of Science and Technology, Wuhan, Hubei 430074, P. R. China*; Email: yuntian@hust.edu.cn

Wei Liu − *College for Advanced Interdisciplinary Studies, National University of Defense Technology, Changsha, Hunan 410073, P. R. China*; orcid.org/0000-0002-7067-6239; Email: wei.liu.pku@gmail.com

Authors

Weijin Chen − *School of Optical and Electronic Information, Huazhong University of Science and Technology, Wuhan, Hubei 430074, P. R. China*

Qingdong Yang − *School of Optical and Electronic Information, Huazhong University of Science and Technology, Wuhan, Hubei 430074, P. R. China*

Complete contact information is available at: https://pubs.acs.org/10.1021/acsomega.0c01843

Author Contributions

‖W.C. and Q. Y. contributed equally to this work.

Notes

The authors declare no competing financial interest.

ACKNOWLEDGMENTS

The authors acknowledge financial support from National Natural Science Foundation of China (Grant nos. 11874026, 11404403, and 11874426) and the Outstanding Young

Researcher Scheme of National University of Defense Technology.

REFERENCES

(1) Bohren, C. F.; Huffman, D. R. *Absorption and Scattering of Light by Small Particles*; Wiley, 1998.
(2) Doicu, A.; Wriedt, T.; Eremin, Y. A. *Light Scattering by Systems of Particles: Null-Field Method with Discrete Sources: Theory and Programs*; Springer, 2006; Vol. *124*.
(3) Gouesbet, G.; Gréhan, G. *Generalized Lorenz-Mie Theories*; Springer Science & Business Media, 2011.
(4) Ferrari, M. Cancer Nanotechnology: Opportunities and Challenges. *Nat. Rev. Cancer* **2005**, *5*, 161−171.
(5) Dreaden, E. C.; Alkilany, A. M.; Huang, X.; Murphy, C. J.; El-Sayed, M. A. The Golden Age: Gold Nanoparticles for Biomedicine. *Chem. Soc. Rev.* **2012**, *41*, 2740−2779.
(6) Alu, A.; Engheta, N. Cloaking a Sensor. *Phys. Rev. Lett.* **2009**, *102*, No. 233901.
(7) Ruan, Z. C.; Fan, S. H. Superscattering of Light from Subwavelength Nanostructures. *Phys. Rev. Lett.* **2010**, *105*, No. 013901.
(8) Qian, C.; Lin, X.; Yang, Y.; Xiong, X.; Wang, H.; Li, E.; Kaminer, I.; Zhang, B.; Chen, H. Experimental Observation of Superscattering. *Phys. Rev. Lett.* **2019**, *122*, No. 063901.
(9) Kerker, M.; Wang, D. S.; Giles, C. L. Electromagnetic Scattering by Magnetic Spheres. *J. Opt. Soc. Am.* **1983**, *73*, No. 765.
(10) Liu, W.; Kivshar, Y. S. Generalized Kerker Effects in Nanophotonics and Meta-Optics [Invited]. *Opt. Express* **2018**, *26*, 13085−13105.
(11) Jahani, S.; Jacob, Z. All-dielectric metamaterials. *Nat. Nanotechnol.* **2016**, *11*, 23−26.
(12) Kuznetsov, A. I.; Miroshnichenko, A. E.; Brongersma, M. L.; Kivshar, Y. S.; Luk'yanchuk, B. Optically Resonant Dielectric Nanostructures. *Science* **2016**, *354*, No. aag2472.
(13) Won, R. Into the 'Mie-Tronic' Era. *Nat. Photonics* **2019**, *13*, 585−587.
(14) Lu, L.; Joannopoulos, J. D.; Soljacic, M. Topological photonics. *Nat. Photonics* **2014**, *8*, 821−829.
(15) Ozawa, T.; Price, H. M.; Amo, A.; Goldman, N.; Hafezi, M.; Lu, L.; Rechtsman, M. C.; Schuster, D.; Simon, J.; Zilberberg, O.; et al. Topological Photonics. *Rev. Mod. Phys.* **2019**, *91*, No. 015006.
(16) Chen, W.; Chen, Y.; Liu, W. Singularities and Poincaré Indices of Electromagnetic Multipoles. *Phys. Rev. Lett.* **2019**, *122*, No. 153907.
(17) Chen, W.; Chen, Y.; Liu, W. Line Singularities and Hopf Indices of Electromagnetic Multipoles, Laser Photonics Rev. 2020, DOI: 10.1002/lpor.202000049. Preprint: arXiv1904.09910.
(18) Milnor, J. W. *Topology from the Differentiable Viewpoint*; Princeton University Press: Princeton, NJ, 1997.
(19) Needham, T. *Visual Complex Analysis*; Clarendon Press, 1998.
(20) Johnson, P. B.; Christy, R. W. Optical Constants of the Noble Metals. *Phys. Rev. B* **1972**, *6*, No. 4370.
(21) Maier, S. A. *Plasmonics: Fundamentals and Applications*; Springer: New York, 2007.
(22) Jackson, J. D. *Classical Electrodynamics*; Wiley: New York, 1962.
(23) Palik, E. D. *Handbook of Optical Constants of Solids*; Academic Press, 1998; Vol. 3.
(24) Liu, W.; Zhang, J.; Miroshnichenko, A. E. Toroidal Dipole-Induced Transparency in Core-shell Nanoparticles. *Laser Photonics Rev.* **2015**, *9*, 564−570.
(25) Feng, T.; Xu, Y.; Zhang, W.; Miroshnichenko, A. E. Ideal Magnetic Dipole Scattering. *Phys. Rev. Lett.* **2017**, *118*, No. 173901.
(26) Liu, W.; Miroshnichenko, A. E.; Neshev, D. N.; Kivshar, Y. S. Broadband Unidirectional Scattering by Magneto-Electric Core-Shell Nanoparticles. *ACS Nano* **2012**, *6*, 5489−5497.
(27) Hopf, H. *Differential Geometry in the Large: Seminar Lectures New York University 1946 and Stanford University 1956*; Springer, 2003.
(28) Nye, J. F. *Natural Focusing and Fine Structure of Light: Caustics and Wave Dislocations*; CRC Press, 1999.
(29) Gbur, G. J. *Singular Optics*; CRC Press Inc.: Boca Raton, 2016.
(30) Birss, R. R. *Symmetry and Magnetism*, 1st ed.; North-Holland Publishng, 1964.
(31) Galvez, E. J.; Rojec, B. L.; Kumar, V.; Viswanathan, N. K. Generation of Isolated Asymmetric Umbilics in Light's Polarization. *Phys. Rev. A* **2014**, *89*, No. 031801(R).
(32) Kumar, V.; Viswanathan, N. K. In *Is Monstar Topologically the Same as Lemon*, Proceedings of the SPIE 9379, Complex Light and Optical Forces IX, 937909, 2015.
(33) Garcia-Etxarri, A. Optical Polarization Mobius Strips on All-Dielectric Optical Scatterers. *ACS Photonics* **2017**, *4*, 1159−1164.
(34) Linden, S.; Enkrich, C.; Wegener, M.; Zhou, J. F.; Koschny, T.; Soukoulis, C. M. Magnetic response of metamaterials at 100 terahertz. *Science* **2004**, *306*, 1351−1353.
(35) Soukoulis, C. M.; Wegener, M. Past Achievements and Future Challenges in the Development of Three-Dimensional Photonic Metamaterials. *Nat. Photonics* **2011**, *5*, 523−530.
(36) Hentschel, M.; Schäferling, M.; Duan, X.; Giessen, H.; Liu, N. Chiral Plasmonics. *Sci. Adv.* **2017**, *3*, No. e1602735.
(37) Bialynicki-Birula, I.; Bialynicka-Birula, Z. Vortex Lines of the Electromagnetic Field. *Phys. Rev. A* **2003**, *67*, No. 062114.
(38) Berry, M. V. Riemann-Silberstein Vortices for Paraxial Waves. *J. Opt. A: Pure Appl. Opt.* **2004**, *6*, S175−S177.
(39) Berry, M. V. Index Formulae for Singular Lines of Polarization. *J. Opt. A: Pure Appl. Opt.* **2004**, *6*, No. 675.
(40) Grahn, P.; Shevchenko, A.; Kaivola, M. Electromagnetic Multipole Theory for Optical Nanomaterials. *New J. Phys.* **2012**, *14*, No. 093033.
(41) Chen, W.; Chen, Y.; Liu, W. Multipolar Conversion Induced Subwavelength High-Q Kerker Supermodes with Unidirectional Radiations. *Laser Photonics Rev.* **2019**, *13*, No. 1900067.

https://dx.doi.org/10.1021/acsomega.0c01843
ACS Omega 2020, 5, 14157−14163